energy&fuels

ARTICLE

pubs.acs.org/EF

CO_2 Capture over $K_2CO_3/MgO/Al_2O_3$ Dry Sorbent in a Fluidized Bed

Lei Li,[†,‡] Yong Li,[†,‡] Xia Wen,[†] Feng Wang,[†] Ning Zhao,[†] Fukui Xiao,[†] Wei Wei,[*,†] and Yuhan Sun[*,†,§]

[†]State Key Laboratory of Coal Conversion, Institute of Coal Chemistry, Chinese Academy of Sciences, Taiyuan 030001, People's Republic of China

[‡]Graduate University of the Chinese Academy of Sciences, Beijing 100049, People's Republic of China

[§]Low Carbon Conversion Center, Shanghai Advanced Research Institute, Chinese Academy of Sciences, Shanghai 201203, People's Republic of China

ABSTRACT: CO_2 capture was carried out over dry $K_2CO_3/MgO/Al_2O_3$ sorbent in a fluidized-bed reactor. The result showed that the total CO_2 adsorption capacity of the new sorbent reached 109.6 mg of CO_2/g of sorbent in the bubbling regime at 60 °C. The X-ray diffraction (XRD) results revealed that there were several kinds of carbonates formed during CO_2 adsorption, such as $KHCO_3$, $KAl(CO_3)_2(OH)_2$, $K_2Mg(CO_3)_2$, $K_2Mg(CO_3)_2 \cdot 4H_2O$, and $MgCO_3$. The high concentration CO_2 could be obtained by the multistage adsorption/desorption cycles. The sorbent could be completely regenerated at 480 °C, and the adsorption capacity remained unchanged after 6 cycles. Furthermore, the application of a conceptual CO_2-capture process using this sorbent was proposed for an existing coal-fired power plant.

1. INTRODUCTION

Carbon capture and storage (CCS) is recognized as a promising option for CO_2 emission reduction.[1−6] The postcombustion process is more suitable for CO_2 capture for the traditional pulverized coal power plants.[6−9] Until now, several processes have been studied for the postcombustion carbon-capture process, such as absorption with a solvent, adsorption using molecular, membrane separation, and cryogenic fractionation. However, these methods need to overcome the limits of cost and consume a lot of energy.[10,11] As a result, CO_2 chemical sorption using dry regenerable alkali-metal-based solid sorbents has been proposed as an innovative concept for CO_2 removal. Alkali metal carbonates (K_2CO_3 or Na_2CO_3) could be used as a sorbent, which reacts with CO_2 and H_2O to form alkali hydrogen carbonates.[7,10−25] Researchers have also tried to develop the K-based sorbents supported on various supports, such as activated carbon, TiO_2, MgO, ZrO_2, Al_2O_3, CaO, SiO_2, and zeolites. The results of CO_2 sorption capacities over different K-based sorbents is summerized in Table 1.[11−13,16,21−25] Among various supports, MgO-supported K_2CO_3 could adsorb a large amount of CO_2 at low temperatures.[11,21] However, the experimental conditions were different from industrial applications (8−17 vol % steam and 10−15 vol % CO_2 in flue gases of a coal-fired power plant), and the carbonation reaction rate was rather slow.[26,27] Recently, Zhao et al. reported that K_2CO_3 calcined from $KHCO_3$ with a hexagonal structure showed a fast rate of carbonation reaction.[26−28] Nevertheless, the mechanical strength of the K_2CO_3/Al_2O_3 sorbent (314 N/cm^2) was not high, which limits its industrial application. The CO_2-capture capacities were also overestimated because they used thermogravimetric analysis (TGA) for CO_2 analysis, which cannot differentiate between CO_2 and H_2O.

In our previous paper, it was found that the MgO/Al_2O_3 sorbent at 10 wt % MgO loading showed better performance for CO_2 capture at low temperatures in the fixed-bed reactor.[29] However, the CO_2 adsorption capacity (59.8 mg of CO_2/g of sorbent) needs to be further improved. Furthermore, in the fixed-bed reactor, heat control is difficult because the adsorption process is highly exothermic. High superficial velocity is necessary to reduce the reactor size. To solve these problems, a fluidized bed is proposed as a proper process to control high volumes of flue gases.[9−13] Thus, in the present work, a new sorbent, MgO/Al_2O_3-supported K_2CO_3, was prepared. The physical properties of the sorbent, such as pore size, pore volume, and surface area, were measured by nitrogen adsorption, and mechanisms of the adsorption and desorption were investigated with the aid of powder X-ray diffraction (XRD) and temperature-programmed desorption (TPD). The performance for CO_2 capture was investigated in the fluidized bed. The parameters, such as pressure drop, gas velocity, and adsorption temperature, were also studied.

2. EXPERIMENTAL SECTION

2.1. Material Preparation. The sorbent used in this study was prepared by the impregnation method. The preparation method of the MgO/Al_2O_3 support (10 wt % MgO) and its microscopic structure were reported in a previous paper.[29] The new sorbent was prepared by impregnating K_2CO_3 on MgO/Al_2O_3 using a wet muti-step impregnating method. Reagent-grade $KHCO_3$ was supplied by Tianjin Fuchen Chemical Reagents Factory. The preparation procedure of the sorbent consisted of three steps: mixing and impregnation, drying at 110 °C for 12 h, and then calcining the solid product in a furnace under N_2 flow (20 mL/min) at 400 °C for 4 h. The sorbent was denoted as KMgAlI3010, where K represents K_2CO_3, I represents the impregnation method, and 30 and 10 represent the loading of K_2CO_3 and MgO, respectively. In comparison, the sorbent without MgO was prepared by the same method and was denoted as KMgAlI3000.

Received: April 2, 2011
Revised: July 4, 2011
Published: July 06, 2011

ACS Publications © 2011 American Chemical Society

Table 1. CO_2 Sorption Capacities over K-Based Sorbents from the Literature

material	temperature (°C)	conditions	total capacity (mg of CO_2/g of sorbent)	method[a]	adsorber	regenerator temperature (°C)	reference
K_2CO_3/AC[b]	60	CO_2, 1 vol %; H_2O, 9 vol %; 40 mL/min	86.0	TCD	fixed bed	150	11
K_2CO_3/Al_2O_3	60	CO_2, 1 vol %; H_2O, 9 vol %; 40 mL/min	85.0	TCD	fixed bed	350	11
K_2CO_3/USY	60	CO_2, 1 vol %; H_2O, 9 vol %; 40 mL/min	18.9	TCD	fixed bed		11
K_2CO_3/CsNaX	60	CO_2, 1 vol %; H_2O, 9 vol %; 40 mL/min	59.4	TCD	fixed bed		11
K_2CO_3/SiO_2	60	CO_2, 1 vol %; H_2O, 9 vol %; 40 mL/min	10.3	TCD	fixed bed		11
K_2CO_3/MgO	60	CO_2, 1 vol %; H_2O, 9 vol %; 40 mL/min	119.0	TCD	fixed bed	400	11
K_2CO_3/CaO	60	CO_2, 1 vol %; H_2O, 9 vol %; 40 mL/min	49.0	TCD	fixed bed		11
K_2CO_3/TiO_2	60	CO_2, 1 vol %; H_2O, 9 vol %; 40 mL/min	83.0	TCD	fixed bed	150	11
K_2CO_3/Al_2O_3	60	CO_2, 1 vol %; H_2O, 9 vol %	86.3	TCD	fixed bed	above 300	22
Re-KAl(I)30[c]	60	CO_2, 1 vol %; H_2O, 9 vol %	82.0	TCD	fixed bed	below 200	22
K_2CO_3/TiO_2	60	CO_2, 1 vol %; H_2O, 9 vol %; 40 mL/min	90.0	TCD	fixed bed	200	23
K_2CO_3/MgO	60	CO_2, 1 vol %; H_2O, 11 vol %	131.3	TCD	fixed bed	350−400	21
K_2CO_3/ZrO_2	50	CO_2, 1 vol %; H_2O, 9 vol %	91.6	TCD	fixed bed	130−200	24
K_2CO_3/Al_2O_3	60	CO_2, 13 vol %; H_2O, 13 vol %; 2.3 m^3/h		TGA	fluidized bed	350	12
sorbKX35[d]	70	CO_2, 14.4 vol %; H_2O, 7 vol %; 60 mL/min	90.0	TGA	fluidized bed	150−230	13
sorbKX35[d]	60	CO_2, 10 vol %; H_2O, 12.2 vol %; 2900 mL/min	111.4	gas analyzer	fluidized bed	300	16,25

[a] TCD, thermal conductivity detector; TGA, thermogravimetric analysis. [b] Activated carbon. [c] Modified K_2CO_3/Al_2O_3 sorbent. [d] Commercial sorbent (K_2CO_3, 35 wt %; supporters, 65 wt %).

2.2. Material Characterization. TPD of CO_2 was performed in a U-shape quartz tube. Typically, 0.1 g of KMgAlI3010 sorbent saturated with simulated flue gases was swept with flowing argon for 1 h at 50 °C to remove the weakly adsorbed CO_2. Then, the temperature was increased from 50 to 600 °C with a heating rate of 10 °C/min under argon flow at 50 mL/min. The CO_2 concentration was monitored by an AMETEK mass spectrometer.

The elemental analysis was performed using the inductively coupled plasma (ICP)−optical emission spectrometer, Perkin-Elmer 3000 equipment.

The structural change of sorbents before/after adsorption was examined by XRD. The XRD analysis was performed on a Bruker D8 Advance X-ray diffractometer with a Cu Kα source at 40 kV and 40 mA. The surface area of the sorbent was determined by nitrogen adsorption with the Brunauer−Emmett−Teller (BET) method on a Micromeritics ASAP-2020 instrument. The pore volume and pore size distribution were obtained with the Bopp−Jancso−Heinzinger method from the adsorption isotherm.

The crushing strength of the sorbent was measured by a digital crushing strength tester (Jiangyan Global Instrument Factory KC-3C), which was a dynamometer measuring the force progressively applied to the solid object during the advancement of a piston. The applied force increases until the solid breaks and collapses into small pieces and eventually powder. The corresponding value of the collapsing force is defined as the crush strength.[29] The detailed properties of KMgAlI3010 and KMgAlI3000 sorbents are shown in Table 2.

2.3. Apparatus and Operation Description. Figure 1 shows the flowchart of the fluidized-bed experimental system, which mainly consists of three subsystems: the gas injection system, fluidized-bed adsorption system, and CO_2 analysis system. The fluidized-bed riser is a 0.650 m tall stainless-steel pipe with an inner diameter of 0.045 m, and the lower mixing zone is a 1.210 m tall stainless-steel pipe with an inner diameter of 0.108 m. Temperatures along the riser are measured at six different points by E-type thermocouples at the height of 300, 630, 760, 920, 1250, and 1580 mm from the distributor plate. The differential pressure in the riser is measured by the pressure sensor (Testo, Germany).

Table 2. Texture Properties of KMgAlI3010 and KMgAlI3000 Sorbents

property	KMgAlI3010	KMgAlI3000
BET surface area (m^2/g)[a]	51.89	75.24
pore space (cm^3/g)[a]	0.27	0.37
average pore diameter (nm)[a]	21.05	19.55
crushing strength (N/cm^2)[b]	998.0	963.0
K_2CO_3/KMgAlI3010 (wt %)[c]	25.43	27.95

[a] Measured by a nitrogen adsorption BET method. [b] Measured by a digital crushing strength tester. [c] Measured by an ICP−optical emission spectrometer.

Dependent upon fuel composition, operating conditions, and the type of coal burned, the composition of flue gases in coal-fired power plants is expected to be approximately 10−15 vol % CO_2,[1,30−32] 8−17 vol % H_2O,[17,18,33] 4−5 vol % O_2, N_2, and trace quantities of other gas species (SO_x and NO_x).[32] A simulated flue gas composition of 10 vol % CO_2, 12 vol % H_2O, and 78 vol % air was used in this study. The steam was introduced by passing the air through a temperature-controlled gas bubbler containing water, and the feed pipeline was heated to avoid H_2O condensation. The H_2O concentration was analyzed by a relative humidity analyzer (Vaisala, Finland). For steam pretreatment, only air passed through the gas bubbler, and as a result, the sorbent adsorbed a certain amount of H_2O before adsorption of CO_2. In the adsorption step, the simulated flue gases entered the fluidized-bed lower mixing zone from a perforated distributor and CO_2 in the flue gases was captured by solid sorbents in a riser where sorbent particles and flue gases were well-mixed with concurrent flow. The flow was monitored by the rotameters located at the inlet of the column. The outlet stream first flowed through a condenser to remove H_2O, then passed through a filter to remove the dust and, finally, passed through a gas analyzer (Vaisala, Finland) to analyze the CO_2 concentration online.

Desorption and purge processes were conducted in a fixed-bed heat regenerator (16 mm in inner diameter and 250 mm in length). A small

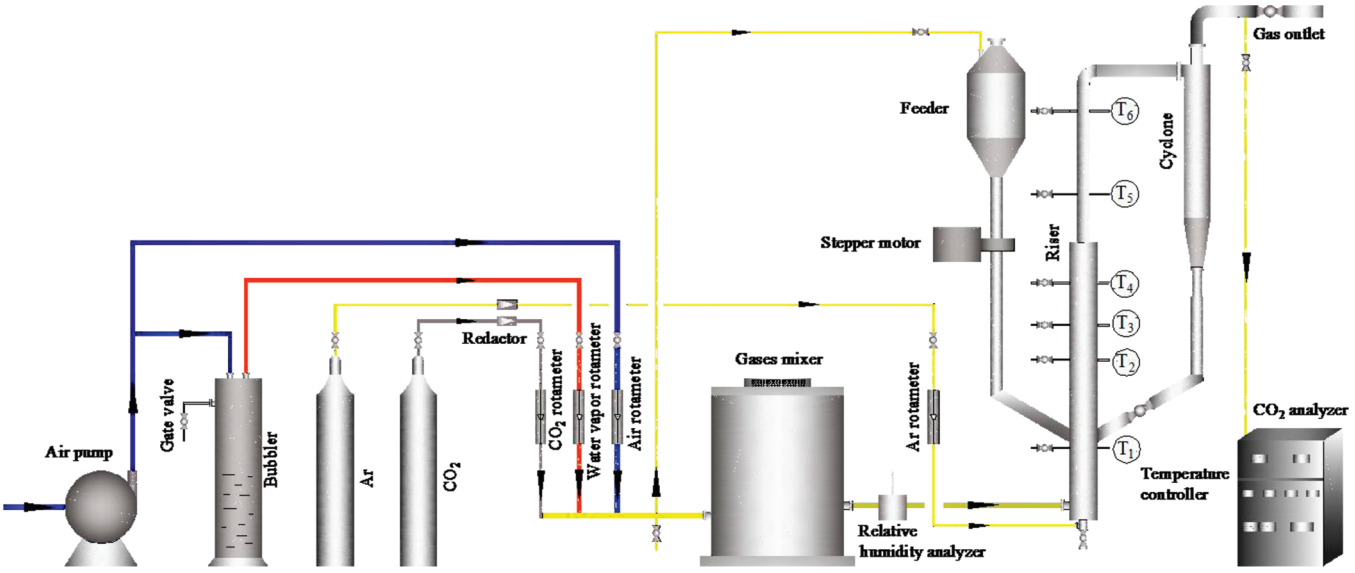

Figure 1. Flowchart of the fluidized-bed experimental apparatus.

Table 3. Experimental Conditions and Results[a]

run	temperature (°C)	flow (m^3/h)	total time (min)	total capacity (mg of CO_2/g of sorbent)	breakthrough time (min)	breakthrough capacity (mg of CO_2/g of sorbent)
1	60	12	10	109.6	2.83	78.3
2	60	22	10	84.5	1.67	60.3
3	60	32	10	59.8	1.00	52.4
4	75	12	10	101.2	2.67	66.0
5	90	12	10	98.1	2.58	65.6
6	60	12	10	77.0	1.83	43.5

[a] Runs 1−5, KMgAlI3010 sorbent; run 6, KMgAlI3000 sorbent; temperature, adsorption temperature; total time, absorption time to reach total capacity; breakthrough time, absorption time to reach breakthrough capacity; feed gas, 10 vol % CO_2, 12 vol % H_2O, and 78 vol % air; and mass of the sorbent, 1000 g.

amount of sorbent (7.2 g) saturated with CO_2 in the fluidized bed was packed into the regenerator. In the desorption process, the feed gas was used as a carrier gas. High-concentration CO_2 effluent was obtained because of the desorption of CO_2 at elevated temperatures. The CO_2 concentration was monitored by a gas analyzer (Vaisala, Finland), while a large amount of the KMgAlI3010 sorbent used for adsorption/desorption cycles in the fluidized bed was regenerated in a muffle furnace.

The range of spherical particle sizes for the KMgAlI3010 sorbent is 1.0−1.8 mm, and the average particle size is 1.4 mm. For the sorbent used in this study, the minimum fluidization flow rate is 11.2 N m^3 h^{-1}, which was determined from the plot of the pressure drop. The minimum value of the calculated flow rate from various correlation transitions to the turbulent regime is 35.0 N m^3 h^{-1};[34] therefore, the simulated flue gases passed through the riser at a flow rate between 12 and 32 N m^3 h^{-1}, which is higher than the minimum fluidization flow rate and lower than the transition flow rate to the turbulent regime. The total and breakthrough capacities were determined by the same methods as in a previous paper.[29] In this work, it took a long time (t = 10 min) to saturate the sorbent, and the breakthrough capacity was calculated when the effluent CO_2 concentration reached 5% of its feed concentration. The breakthrough curves showed a gradual increase of the C_{out}/C_{in} ratio from 0 to 1 (C_{out} and C_{in} refer to the CO_2 concentrations in the outlet and inlet flue gases, respectively). The CO_2 sorption capacity was calculated from the CO_2 sorption profile by considering the CO_2 flow profile without any sorbent mounted in the fluidized bed (used as a blank). All of the experimental conditions and results are listed in Table 3, and the run numbers in the following text refer to those listed in the table.

3. RESULTS AND DISCUSSION

3.1. Identification of the Structure of the KMgAlI3010 Sorbent. Figure 2 illustrates the CO_2−TPD profiles of the KMgAlI3010 sorbent. The TPD profile of the KMgAlI3010 sorbent showed five CO_2 desorption peaks, indicating that five kinds of substances were formed after CO_2 adsorption.

Figure 3 shows the XRD patterns of fresh sorbent, sorbent pretreated with H_2O, and sorbent after CO_2 adsorption. As can be seen, only K_2CO_3 (PDF 27-1348) and Al_2O_3 (PDF 29-0063) phases were found for the fresh sample (Figure 3a). It might be because MgO was highly dispersed on the internal surfaces of the mesopores in the samples, which is accordance with the previous study.[29] After pretreatment with H_2O for 1 h, $K_4H_2(CO_3)_3\cdot 1.5H_2O$ (PDF 20-0886) was the most abundant phase, while the peak intensity of $K_2CO_3\cdot 1.5H_2O$ (PDF 11-0655) was quite weak (Figure 3b). The $K_4H_2(CO_3)_3\cdot 1.5H_2O$ phase was considered as the main active species for capturing CO_2.[26−28] The XRD pattern of the sorbent after CO_2 adsorption at 60 °C

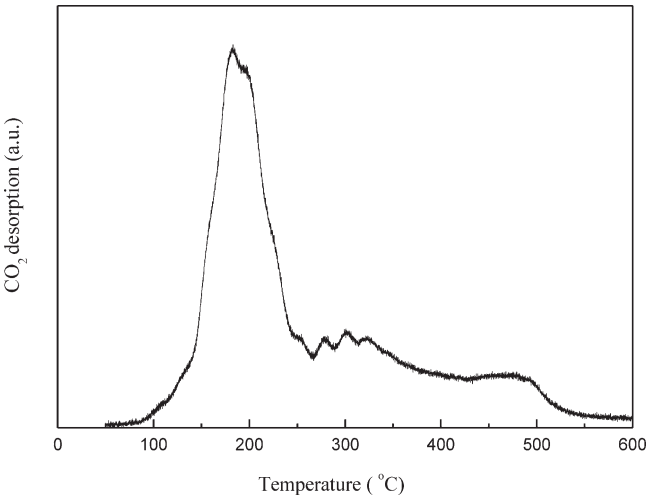

Figure 2. CO_2—TPD profiles of the KMgAlI3010 sorbent.

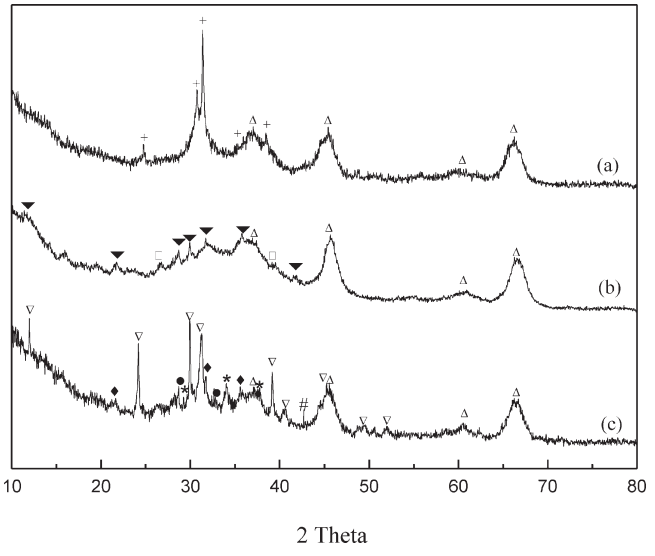

Figure 3. XRD patterns of the KMgAlI3010 sorbent (a) before, (b) after the pretreatment with 12 vol % of steam for 1 h, and (c) after adsorption with simulated flue gases at 60 °C: +, K_2CO_3; △, Al_2O_3; ▼, $K_4H_2(CO_3)_3 \cdot 1.5H_2O$; □, $K_2CO_3 \cdot 1.5H_2O$; ▽, $KHCO_3$; ◆, $KAl(CO_3)_2(OH)_2$; ●, $K_2Mg(CO_3)_2$; ★, $K_2Mg(CO_3)_2 \cdot 4H_2O$; and #, $MgCO_3$.

showed five phases (Figure 3c): $KHCO_3$ (PDF 12-0292), $KAl(CO_3)_2(OH)_2$ (PDF 21-0979), $K_2Mg(CO_3)_2 \cdot 4H_2O$ (PDF 29-1017), $K_2Mg(CO_3)_2$ (PDF 33-1495), and $MgCO_3$ (PDF 08-0479).

3.2. CO_2 Adsorption in the Fluidized Bed. Figure 4 shows the bed temperature profiles at different heights of the fluidized bed. The bed was preheated by hot air for 40 min to reach the desired temperature. After the sorbent (1000 g) was introduced into the fluidized bed, the bed temperature decreased first, then increased, and reached the pretreatment temperature (around 60 °C). The axial temperature gradient of the bed was very small, which indicated that the fluidized bed had excellent heat-transfer efficiency. Then, the gas flow was switched to air containing 12 vol % H_2O and maintained at 60 °C for 40 min to activate the sorbent. After that, the gas flow was switched to the simulated flue gases. Some variations in the temperature across the fluidized

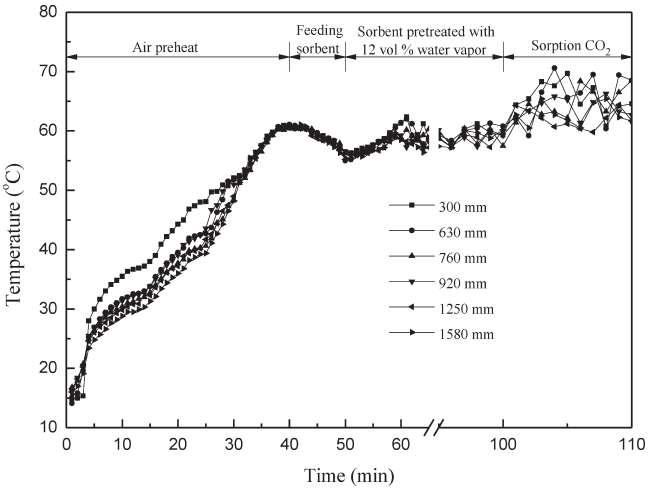

Figure 4. Bed temperature distribution at different heights of the fluidized bed.

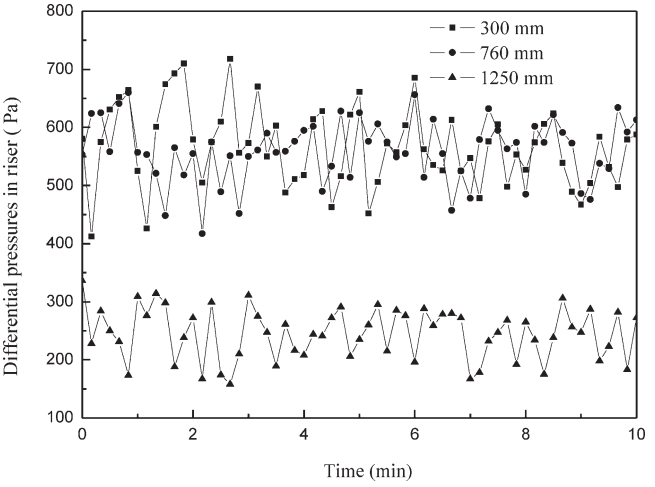

Figure 5. Axial differential pressure profile of the fluidized bed during the sorption process. Flow rate, 12 N m^3 h^{-1}; amount of sorbent, 1000 g.

bed were observed because of the exothermic nature of the adsorption.[35,36]

The pressure drop profiles at three different positions in the fluidized bed were also monitored during the sorption process, as shown in Figure 5. The differential pressures at three positions were about 570, 560, and 250 Pa, respectively, from the bottom to the top section. These results might provide valuable data to estimate the design of fan power.[13]

To investigate the effect of the flow rate of flue gases, the breakthrough curves of CO_2 were measured at a flow rate between 12 and 32 N m^3 h^{-1}. Figure 6 illustrates the CO_2 concentrations in the outlet stream against the adsorption time under different flow rates. Both total and breakthrough capacities of CO_2 adsorption are listed in Table 3 (runs 1—3). It can be seen that CO_2 was completely removed from the flue gases in the early stage (1—2 min) because no CO_2 was detected in the outlet stream. Then, the CO_2 concentration in the outlet stream gradually increased to the feeding level in the next 2—5 min. While, in a blank experiment, the C_{out}/C_{in} ratio quickly recovered to 1 when there is no sorbent placed in the fluidized bed. As

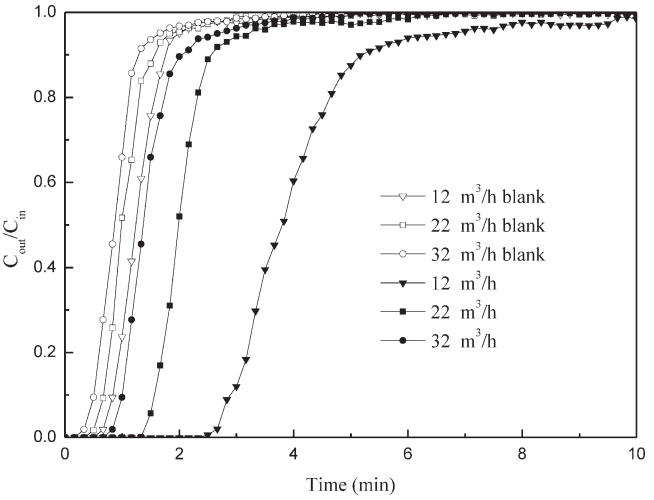

Figure 6. Breakthrough curves of CO_2 against the adsorption time at various flow rates. Adsorption temperature, 60 °C; feed gas, 10 vol % CO_2, 12 vol % H_2O, and 78 vol % air; and amount of sorbent, 1000 g.

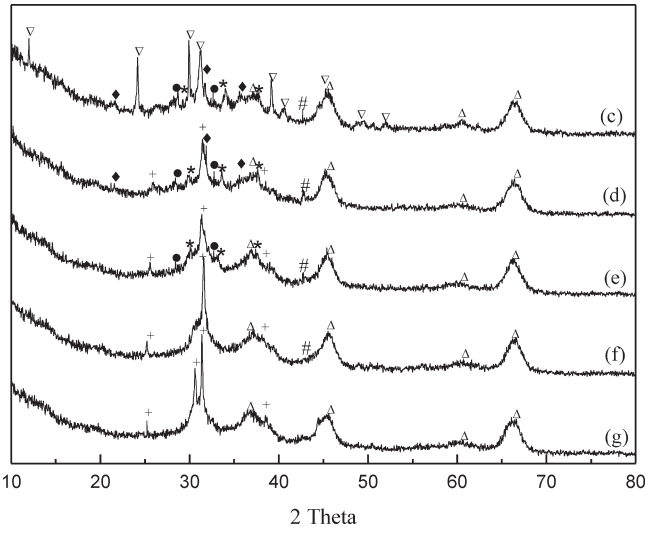

Figure 7. Sorbent regenerated under nitrogen at various temperatures, such as (d) 180 °C, (e) 300 °C, (f) 400 °C, and (g) 480 °C: +, K_2CO_3; △, Al_2O_3; ▽, $KHCO_3$; ◆, $KAl(CO_3)_2(OH)_2$; ●, $K_2Mg(CO_3)_2$; ★, $K_2Mg(CO_3)_2 \cdot 4H_2O$; and #, $MgCO_3$.

seen from Figure 6, a shift of breakthrough curves to a shorter time was observed at a higher flow rate, which indicated that the CO_2 adsorption capacity of the sorbent was saturated faster as the space time of the feed gases increased.[13] In comparison, KMgAlI3010 captured more CO_2 at the flow rate of 12 N m^3 h^{-1} than at a higher flow rate. CO_2 captured was 109.6 mg of CO_2/g of KMgAlI3010 sorbent, which was calculated by integrating the area between the adsorption curve and the blank curve. However, the CO_2 capacity of the KMgAlI3000 sorbent was 77.0 mg of CO_2/g of sorbent at the same experimental conditions (run 6 in Table 3). From these results, it could be concluded that MgO played an important role in the high CO_2-capture capacity of the KMgAlI3010 sorbent. It might be because MgO not only participated directly in CO_2 adsorption but also could help K_2CO_3 transform to $K_2Mg(CO_3)_2 \cdot 4H_2O$ and $K_2Mg(CO_3)_2$.[11,21]

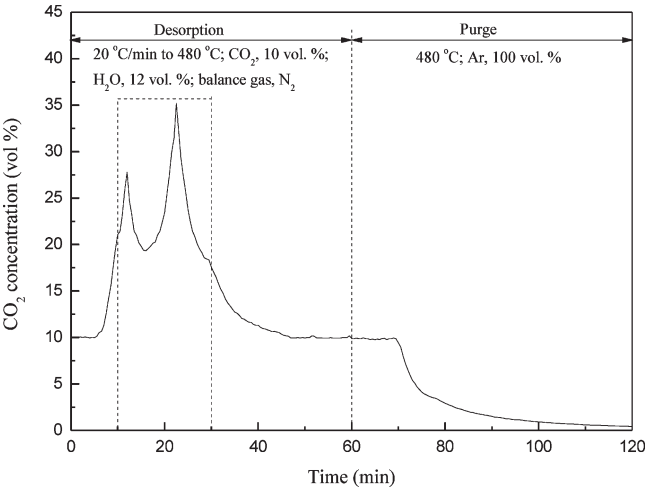

Figure 8. CO_2 concentration change during the desorption and purge cycle in the fixed-bed heat regenerator. Adsorption temperature, 60 °C; pressure, 101 325 Pa; flow rate, 80 mL/min; balance gas, N_2; and amount of KMgAlI3010 sorbent, 7.2 g.

The effect of the adsorption temperature on the capacity of CO_2 adsorption was also investigated. Both total and breakthrough adsorption capacities of CO_2 are listed in runs 1, 4, and 5 of Table 3. Clearly, the total adsorption capacities of CO_2 were 109.6, 101.2, and 98.1 mg of CO_2/g of sorbent at 60, 75, and 90 °C, respectively. The adsorption capacity of CO_2 decreased as the adsorption temperature increased because both physical and chemical adsorption (usually) were exothermic.[35,36] Even though a lower temperature is favorable for the carbonation reaction, the process should be operated above the dew point of H_2O to prevent water condensation.

To identify the properity of the substances formed after CO_2 adsorption, the XRD patterns of the sorbents were collected after regeneration at various temperatures, e.g., 180, 300, 400, and 480 °C (Figure 7). As the temperature increased to 180 °C, the phase of $KHCO_3$ disappeared (Figure 7d).[11,15,21,37−41] The diffraction peaks of $KAl(CO_3)_2(OH)_2$ gradually decreased with the temperature increase and disappeared completely at 300 °C, which indicated that $KAl(CO_3)_2(OH)_2$ was completely converted to K_2CO_3 at 300 °C (Figure 7e),[11,15,22,37] while $K_2Mg(CO_3)_2 \cdot 4H_2O$ and $K_2Mg(CO_3)_2$ were found to completely decompose to K_2CO_3 at temperatures of 300−400 °C (Figure 7f). After regeneration at 480 °C in nitrogen, $MgCO_3$ was completely converted to MgO (Figure 7g). It was consistent with the structure of the MgO/Al_2O_3 sorbent after adsorption of CO_2, which was ascribed to unidentate carbonate species.[29] However, no diffraction peaks of MgO were observed, which might be because of the low MgO loading. The XRD profiles in Figures 3a and 7g were almost the same, which indicated that the sorbent could be completely regenerated at 480 °C. These results were well in agreement with the TPD result.

3.3. Regeneration of the Sorbent. Besides the CO_2-capture capacity, the regeneration property is also one of the most important factors that affect the application of the sorbent. A total of 7.2 g of the saturated KMgAlI3010 sorbents (exposed to CO_2 in the flue gases at 60 °C, with a flow rate of 12 N m^3 h^{-1}) was regenerated in the fixed-bed heat regenerator. Although pure CO_2 could be used for desorption in the actual situation, a relatively high concentration of CO_2 also could be obtained using

the feed gases as a carrier. Figure 8 shows the CO_2 concentration change in the desorption and purge processes. The test was carried out by measuring the concentration of CO_2 desorbed when the temperature ramping rate was 20 °C/min from 60 to 480 °C. There were two main desorption peaks of CO_2. One was attributed to $KHCO_3$, and the other one, which was a composite peak, could be ascribed to other carbonates. This result was inconsistent with the CO_2−TPD results, which might have originated from the different CO_2 analyzer used in the regeneration cycle. As shown in Figure 8, the average concentration of CO_2 desorbed in the desorption process increased from 10 to 25 vol %, which indicated that a higher concentration of CO_2 could be obtained by the multi-stage adsorption/desorption cycles. In the purge process, the sorbent was purged in argon at 480 °C for 60 min, during which the KMgAlI3010 sorbent could be completely regenerated. However, in practice, any CO_2-capture process might not need complete regeneration. As seen from the CO_2−TPD results (Figure 2), about 80% of CO_2 was released below 350 °C, so that the regeneration temperature of 350 °C might be sufficient for sorbent recycle.

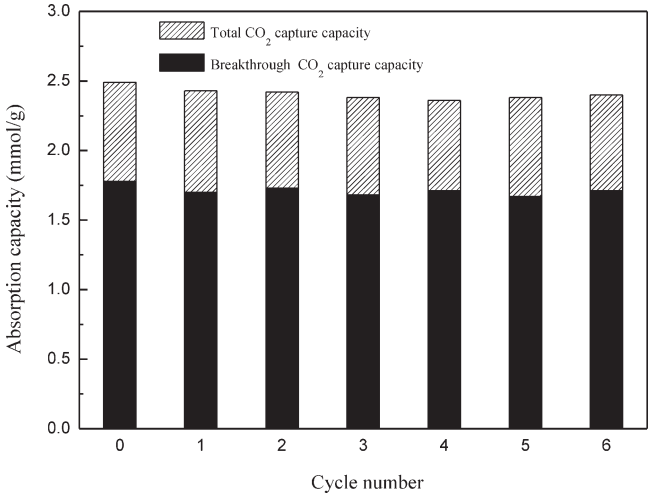

Figure 9. Total and breakthrough capacities of CO_2 over the KMgAlI3010 sorbent for multiple adsorption/desorption cycles in the fluidized bed. Flow rate, 12 N m^3 h^{-1}; feed gas, 10 vol % CO_2, 12 vol % H_2O, and 78 vol % air; balance gas, air; regeneration temperature, 480 °C; and amount of KMgAlI3010 sorbent, 1000 g.

For commercial application, the sorbent should not only possess high capacity and high selectivity but also exhibit stable performance over multiple adsorption/desorption cycles.[29] In this study, the sorbent used for adsorption/desorption cycles in the fluidized bed was regenerated under N_2 flow (20 mL/min) at 480 °C for 3 h in a muffle furnace. Figure 9 shows the total and breakthrough capacities of CO_2 over the KMgAlI3010 sorbent for 6 adsorption/desorption cycles in the fluidized bed. The stable adsorption/desorption performance suggests the sorbent is promising for practical applications.

3.4. Process Considerations. A block flow diagram of the conceptual KMgAlI3010 sorbent CO_2-capture process in a coal-fired power plants is thus proposed in Figure 10. After the electrostatic precipitator, the hot flue gases (350−400 °C) enter a denitrification unit. Through the heat exchanger, the temperature of the flue gases decrease to 130−160 °C. Then, the gases pass through a desulfurization unit. After the desulfurization unit, the temperature of the flue gases decreases to 50−100 °C. Desulfurized flue gases are then introduced into the carbonator, where CO_2 reacts with the sorbent and forms carbonates. The carbonator, regenerator, and activator system are visualized as fluidized beds. The cooling system located at the bottom of the carbonator can remove the adsorption heat to ensure the stable operation of the system. Flue gases with lower CO_2 concentrations are separated from partially reacted sorbent and then discharged. A portion of the partially reacted sorbent is recycled, and the other parts are transferred to the regenerator. At the regeneration stage, the steam or pure CO_2 can be used as carrier

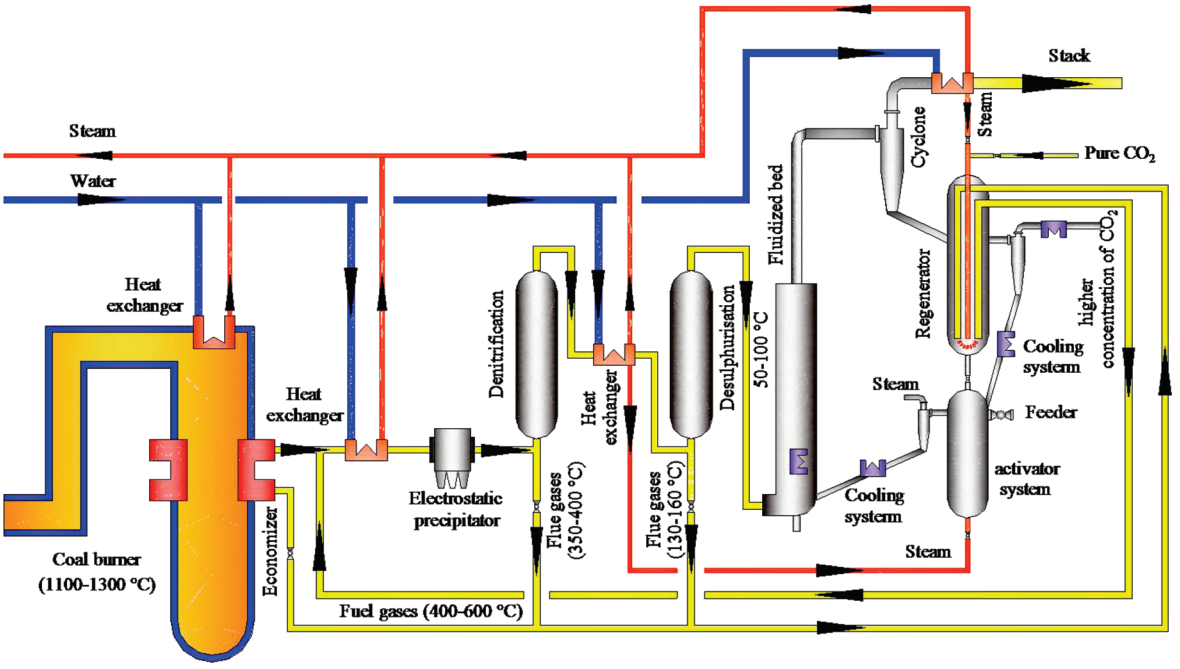

Figure 10. Block flow diagram of the conceptual KMgAlI3010 sorbent CO_2-capture process in coal-fired power plants.

dx.doi.org/10.1021/ef200499b |*Energy Fuels* 2011, 25, 3835–3842

gases. The hot flue gases from different sections of coal-fired power plants or a part of superheated steam could be used as the source of heat to regenerate the sorbent. For example, the KMgAlI3010 sorbent can be regenerated by the hot flue gases (400−600 °C) from an economizer.[5,41] Regenerated sorbent is mixed with the fresh sorbent in the activator system. The sorbent is pretreated with steam to form active species and then transfers back to the carbonator. The pure CO_2 product is ready for other applications or sequestration.

4. CONCLUSION

Experiments on CO_2 capture in the fluidized bed showed that the KMgAlI3010 sorbent had a high CO_2 uptake of 109.6 mg of CO_2/g of sorbent at the flow rate of 12 N m^3 h^{-1} at 60 °C under simulated flue gas conditions, which was larger than those of most K-based sorbents reported before at low temperatures. MgO played an important role in the high CO_2-capture capacity of the KMgAlI3010 sorbent. During the CO_2 adsorption process, several kinds of carbonates formed, including $KHCO_3$, $KAl(CO_3)_2(OH)_2$, $K_2Mg(CO_3)_2$, $K_2Mg(CO_3)_2 \cdot 4H_2O$, and $MgCO_3$. High concentrations of CO_2 could be obtained by the multistage adsorption/desorption cycles, during which the KMgAlI3010 sorbent could be completely regenerated at 480 °C. In addition, the sorbent had high mechanical strength and exhibited good stability in 6 cycles.

AUTHOR INFORMATION

Corresponding Author

*Telephone: +86-351-4049612. Fax: +86-351-4041153. E-mail: weiwei@sxicc.ac.cn (W.W.); yhsun@sxicc.ac.cn (Y.S.).

ACKNOWLEDGMENT

This work was supported by the Lu'an Group, the Knowledge Innovation Programme of the Chinese Academy of Science (KGCX2-YW-323), the Ministry of Science and Technology of the People's Republic of China (2009BWZ003), and the National Natural Science Foundation of China (50976116).

REFERENCES

(1) Mikkelsen, M.; Jørgensen, M.; Krebs, F. C. The teraton challenge. A review of fixation and transformation of carbon dioxide. *Energy Environ. Sci.* **2010**, *3* (1), 43–81.

(2) Soares, J. L.; Oberziner, A. L. B.; José, H. J.; Rodrigues, A. E.; Moreira, R. F. P. M. Carbon dioxide adsorption in Brazilian coals. *Energy Fuels* **2007**, *21* (1), 209–215.

(3) Belmabkhout, Y.; Sayari, A. Isothermal versus non-isothermal adsorption−desorption cycling of triamine-grafted pore-expanded MCM-41 mesoporous silica for CO_2 capture from flue gas. *Energy Fuels* **2010**, *24*, 5273–5280.

(4) Drage, T. C.; Blackman, J. M.; Pevida, C.; Snape, C. E. Evaluation of activated carbon adsorbents for CO_2 capture in gasification. *Energy Fuels* **2009**, *23*, 2790–2796.

(5) Xiong, R. T.; Ida, J.; Lin, Y. S. Kinetics of carbon dioxide sorption on potassium-doped lithium zirconate. *Chem. Eng. Sci.* **2003**, *58* (29), 4377–4385.

(6) Thiruvenkatachari, R.; Su, S.; An, H.; Yu, X. X. Post combustion CO_2 capture by carbon fibre monolithic adsorbents. *Prog. Energy Combust. Sci.* **2009**, *35* (5), 438–455.

(7) Liang, Y.; Harrison, D. P.; Gupta, R. P.; Green, D. A.; McMichael, W. J. Carbon dioxide capture using dry sodium-based sorbents. *Energy Fuels* **2004**, *18* (2), 569–575.

(8) Qi, G. G.; Wang, Y. B.; Estevez, L.; Duan, X. N.; Anako, N.; Park, A. H. A.; Li, W.; Jones, C. W.; Giannelis, E. P. High efficiency nanocomposite sorbents for CO_2 capture based on amine-functionalized mesoporous capsules. *Energy Environ. Sci.* **2011**, *4* (2), 444–452.

(9) Romeo, L. M.; Abanades, J. C.; Escosa, J. M.; Pano, J.; Gimenez, A.; Sanchez-Biezma, A.; Ballesteros, J. C. Oxyfuel carbonation/calcination cycle for low cost CO_2 capture in existing power plants. *Energy Convers. Manage.* **2008**, *49* (10), 2809–2814.

(10) Park, Y. C.; Jo, S. H.; Park, K. W.; Park, Y. S.; Yi, C. K. Effect of bed height on the carbon dioxide capture by carbonation/regeneration cyclic operations using dry potassium-based sorbents. *Korean J. Chem. Eng.* **2009**, *26* (3), 874–878.

(11) Lee, S. C.; Choi, B. Y.; Lee, T. J.; Ryu, C. K.; Ahn, Y. S.; Kim, J. C. CO_2 absorption and regeneration of alkali metal-based solid sorbents. *Catal. Today* **2006**, *111* (3−4), 385–390.

(12) Zhao, C. W; Chen, X. P.; Zhao, C. S. Multiple-cycles behavior of K_2CO_3/Al_2O_3 for CO_2 capture in a fluidized-bed reactor. *Energy Fuels* **2010**, *24*, 1009–1012.

(13) Yi, C. K.; Jo, S. H.; Seo, Y.; Lee, J. B.; Ryu, C. K. Continuous operation of the potassium-based dry sorbent CO_2 capture process with two fluidized-bed reactors. *Int. J. Greenhouse Gas Control* **2007**, *1* (1), 31–36.

(14) Park, Y. C.; Jo, S. H.; Ryu, C. K.; Yi, C. K. Long-term operation of carbon dioxide capture system from a real coal-fired flue gas using dry regenerable potassium-based sorbents. *Energy Procedia* **2009**, *1* (1), 1235–1239.

(15) Lee, S. C.; Kim, J. C. Dry potassium-based sorbents for CO_2 capture. *Catal. Surv. Asia* **2007**, *11* (4), 171–185.

(16) Seo, Y.; Jo, S. H.; Ryu, H. J.; Bae, D. H.; Ryu, C. K.; Yi, C. K. Effect of water pretreatment on CO_2 capture using a potassium-based solid sorbent in a bubbling fluidized bed reactor. *Korean J. Chem. Eng.* **2007**, *24* (3), 457–460.

(17) Hirano, S.; Shigemoto, N.; Yamada, S.; Hayashi, H. Cyclic fixed-bed operations over K_2CO_3-on-carbon for the recovery of carbon dioxide under moist conditions. *Bull. Chem. Soc. Jpn.* **1995**, *68* (3), 1030–1035.

(18) Hayashi, H.; Taniuchi, J.; Furuyashiki, N.; Sugiyama, S.; Hirano, S.; Shigemoto, N.; Nonaka, T. Efficient recovery of carbon dioxide from flue gases of coal-fired power plants by cyclic fixed-bed operations over K_2CO_3-on-carbon. *Ind. Eng. Chem. Res.* **1998**, *37* (1), 185–191.

(19) Ficicilar, B.; Dogu, T. Breakthrough analysis for CO_2 removal by activated hydrotalcite and soda ash. *Catal. Today* **2006**, *115* (1−4), 274–278.

(20) Park, S. W.; Sung, D. H.; Choi, B. S.; Oh, K. J.; Moon, K. H. Sorption of carbon dioxide onto sodium carbonate. *Sep. Sci. Technol.* **2006**, *41* (12), 2665–2684.

(21) Lee, S. C.; Chae, H. J.; Lee, S. J.; Choi, B. Y.; Yi, C. K.; Lee, J. B.; Ryu, C. K.; Kim, J. C. Development of regenerable MgO-based sorbent promoted with K_2CO_3 for CO_2 capture at low temperarures. *Environ. Sci. Technol.* **2008**, *42* (8), 2736–2471.

(22) Lee, S. C.; Kwon, Y. M.; Ryu, C. Y.; Chae, H. J.; Ragupathy, D.; Jung, S. Y.; Lee, J. B.; Ryu, C. K.; Kim, J. C. Development of new alumina-modified sorbents for CO_2 sorption and regeneration at temperatures below 200 °C. *Fuel* **2011**, *90* (4), 1465–1470.

(23) Lee, S. C.; Kwon, Y. M.; Park, Y. H.; Lee, W. S.; Park, J. J.; Ryu, C. K.; Yi, C. K.; Kim, J. C. Structure effects of potassium-based TiO_2 sorbents on the CO_2 capture capacity. *Top. Catal.* **2010**, *53* (7−10), 641–647.

(24) Lee, S. C.; Chae, H. J; Lee, S. J.; Park, Y. H.; Ryu, C. K.; Yi, C. K.; Kim, J. C. Novel regenerable potassium-based dry sorbents for CO_2 capture at low temperatures. *J. Mol. Catal. B: Enzym.* **2009**, *56* (2−3), 179–184.

(25) Seo, Y.; Jo, S. H.; Ryu, C. K.; Yi, C. K. Effect of reaction temperature on CO_2 capture using potassium-based solid sorbent in bubbling fluidized-bed reactor. *J. Environ. Eng.* **2009**, *13* (6), 473–477.

(26) Zhao, C. W.; Chen, X. P.; Zhao, C. S.; Liu, Y. K. Carbonation and hydration characteristics of dry potassium based sorbents for CO_2 capture. *Energy Fuels* **2009**, *23*, 1766–1769.

(27) Zhao, C. W.; Chen, X. P.; Zhao, C. S. Study on CO_2 capture using dry potassium-based sorbents through orthogonal test method. *Int. J. Greenhouse Gas Control* **2010**, *4* (4), 655–658.

(28) Zhao, C. W.; Chen, X. P.; Zhao, C. S. Effect of crystal structure on CO_2 capture characteristics of dry potassium-based sorbents. *Chemosphere* **2009**, *75* (10), 1401–1404.

(29) Li, L.; Wen, X.; Fu, X.; Wang, F.; Zhao, N.; Xiao, F. K.; Wei, W.; Sun, Y. H. MgO/Al_2O_3 sorbent for CO_2 capture. *Energy Fuels* **2010**, *24*, 5773–5780.

(30) Park, J. H.; Beum, H. T.; Kim, J. N.; Cho, S. H. Numerical analysis on the power consumption of the PSA process for recovering CO_2 from flue gas. *Ind. Eng. Chem. Res.* **2002**, *41* (16), 4122–4131.

(31) Khatri, R. A.; Chuang, S. S. C.; Soong, Y.; Gray, M. Thermal and chemical stability of regenerable solid amine sorbent for CO_2 capture. *Energy Fuels* **2006**, *20* (4), 1514–1520.

(32) Lee, S.; Filburn, T. P.; Gray, M.; Park, J. W.; Song, H. J. Screening test of solid amine sorbents for CO_2 capture. *Ind. Eng. Chem. Res.* **2008**, *47* (19), 7419–7423.

(33) Xu, X. C.; Song, C. S.; Miller, B. G.; Scaroni, A. W. Influence of moisture on CO_2 separation from gas mixture by a nanoporous adsorbent based on polyethylenimine-modified molecular sieve MCM-41. *Ind. Eng. Chem. Res.* **2005**, *44* (21), 8113–8119.

(34) Han, G. Y.; Lee, G. S.; Kim, S. D. Hydrodynamic characteristics of a circulating fluidized bed. *Korean J. Chem. Eng.* **1985**, *2* (2), 141–147.

(35) Ruthven, D. M. *Principles of Adsorption and Adsorption Processes*; John Wiley and Sons, Inc.: New York, 1984.

(36) Atkins, P. W. *Physical Chemistry*; Oxford University Press: Oxford, U.K., 1990.

(37) Lee, S. C.; Choi, B. Y.; Ryu, C. K.; Ahn, Y. S.; Lee, T. J.; Kim, J. C. The effect of water on the activation and the CO_2 capture capacities of alkali metal-based sorbents. *Korean J. Chem. Eng.* **2006**, *23* (3), 374–379.

(38) Okunev, A. G.; Sharonov, V. E.; Aristov, Y. I.; Parmon, V. N. Sorption of carbon dioxide from wet gases by K_2CO_3-in-porous matrix: Influence of the matrix nature. *React. Kinet. Catal. Lett.* **2000**, *71* (2), 355–362.

(39) Sharonov, V. E.; Tyshchishchin, E. A.; Moroz, E. M.; Okunev, A. G.; Aristov, Y. I. Sorption of CO_2 from humid oases on potassium carbonate supported by porous matrix. *Russ. J. Appl. Chem.* **2001**, *74* (3), 409–413.

(40) Okunev, A. G.; Sharonov, V. E.; Gubar, A. V.; Danilova, I. G.; Paukshtis, E. A.; Moroz, E. M.; Kriger, T. A.; Malakhov, V. V.; Aristov, Y. I. Sorption of carbon dioxide by the composite sorbent "potassium carbonate in porous matrix". *Russ. Chem. Bull. Int. Ed.* **2003**, *52* (2), 359–363.

(41) Wang, X. P.; Yu, J. J.; Cheng, J.; Hao, Z. P.; Xu, Z, P. High temperature adsorption of carbon dioxide on mixed oxides derived from hydrotalcite-like compounds. *Environ. Sci. Technol.* **2008**, *42* (2), 614–618.